Int. J. Solids Structures, 1971, Vol. 7, pp. 1127 to 1142. Pergamon Press. Printed in Great Britain

INFLUENCE OF PULSE SHAPE ON THE FINAL PLASTIC DEFORMATION OF A CIRCULAR PLATE†

CARL K. YOUNGDAHL

Engineering and Technology Division, Argonne National Laboratory, Argonne, Illinois 60439

Abstract—A closed-form solution is obtained for the dynamic plastic deformation of a simply-supported circular plate subjected to a pressure pulse of general shape. It is shown that the final plastic deformation is strongly dependent on the pulse shape. However, the effect of the pulse shape can be characterized by an effective pressure defined in terms of simple integrals of the pressure–time function.

1. INTRODUCTION

THE dynamic plastic deformation of a simply supported rigid-plastic circular plate (Fig. 1) subjected to a uniform pressure $P(t)$ having a rectangular pulse shape is treated extensively by Hopkins and Prager [1]. A closed-form solution will be derived here for the general pulse shape given by Fig. 2. It will be shown that the amount of plastic deformation is strongly dependent on the pulse shape for pulses which have the same impulse and maximum pressure; the effect of the pulse shape is eliminated, however, for pulses which have the same impulse and *effective pressure*. The *effective pressure* is defined as the impulse divided by twice the mean time of the pulse, with the mean time being the interval between the onset of plastic deformation and the centroid of the pulse.

Perzyna [2] extended the Hopkins and Prager [1] solution to other pulse shapes and found little influence of the pressure–time function on the final deformation. However, his pulse shapes were initially rectangular followed by various types of decays, so that they were close to the rectangular shape in form and effect. Hodge [3] showed that the dynamic plastic deformation of a reinforced circular cylindrical shell was strongly influenced by the pulse shape for pulses with the same impulse and peak value. Symonds [4] found less pulse-shape dependence for a beam subjected to a dynamic force; however, his results are for maximum loadings which greatly exceed the yield load. The author [5] has shown that the effect of pulse shape on the results of the Hodge and Symonds papers can be eliminated if the pulses have the same impulse and effective value, with the effective value being defined analogously to the effective pressure used here.

Wang [6] investigated the plastic deformation of a simply supported circular plate loaded impulsively. Perrone [7] and Wierzbicki [8] included the effects of strain-rate sensitivity and viscoplasticity, while Jones [9] considered the influence of membrane forces on finite deflections, as well as strain-hardening and strain rate sensitivity. Conroy [10] solved the problem of a simply-supported plate loaded dynamically over a portion of its surface, and Florence [11] treated the corresponding clamped plate problem. Solutions for other clamped plate problems are given by Wang and Hopkins [12], Shapiro

† Work performed under the auspices of the U.S. Atomic Energy Commission.

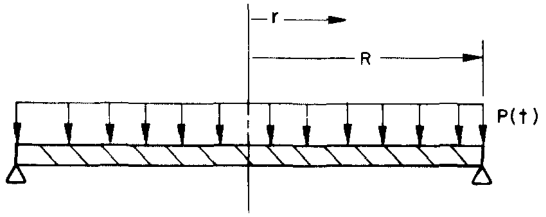

FIG. 1. Circular plate.

[13] and Jones [14, 15]. Experimental results for dynamically loaded, plastically deformed plates are presented by Florence [16], Duffey and Key [17] and Wierzbicki and Florence [18].

The statement of the problem presented in the next section is an abbreviated version of the thorough exposition given by Hopkins and Prager [1]. A closed-form solution for general pulse shapes such that a hinge band is not formed is derived by Perzyna [2] in a somewhat different form from that obtained in Section 3 of this paper. He divides pulses which produce hinge bands into two categories, "blast" and "impact" loads. Blast loads are those that rise instantaneously to their maximum value and decay thereafter, while impact loads attain their maximum in a non-zero time interval. Perzyna derives the differential equation for the hinge circle motion corresponding to blast loads and solves it numerically for two pulse shapes; he does not treat impact loads. A closed-form solution for both types of loads is derived in Section 4 of this paper. (Blast loads may be considered to be a special case of impact loads by letting the rise time of the pulse go to zero.) A closed-form expression for Perzyna's numerical results may be obtained by substitution of his pulse shapes into the solution given here. In Section 5, deformation results for a variety of pulse shapes are presented. It is shown that the effect of the pulse shape on the final plastic deformation is eliminated if the effective pressure is used to characterize the pressure pulse, the effective pressure being defined in terms of the integral of the pulse and its first moment.

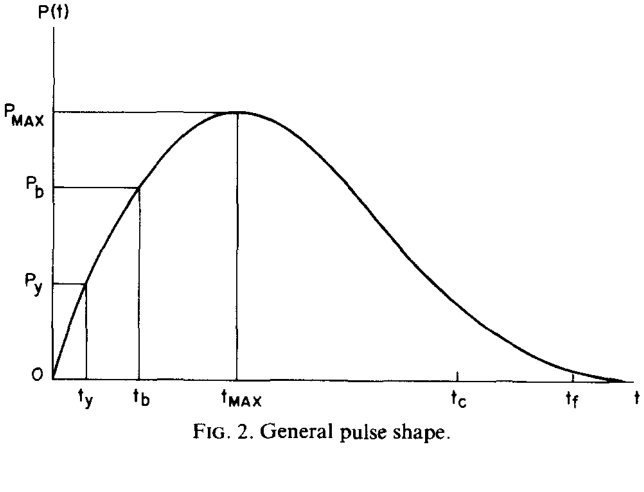

FIG. 2. General pulse shape.

2. STATEMENT OF PROBLEM

Under the usual assumptions of the small deflection theory of thin plates, the equation of motion of the simply supported circular plate of Fig. 1 is

$$\begin{aligned}\frac{\partial}{\partial r}(rM_r) - M_\phi &= rQ \\ &= \int_0^r \left[-P + \mu\frac{\partial^2 W}{\partial t^2}\right] r\,\mathrm{d}r,\end{aligned} \tag{2.1}$$

where M_r, M_ϕ and Q are the radial bending moment, circumferential bending moment and vertical shear force per unit arc length, respectively, P is the applied pressure, μ is the mass per unit surface area and W is the downward deflection of points lying in the middle surface. The quantities M_r, M_ϕ, Q and W are functions of radius r and time t; P will be taken to be a function of time only and may have the general shape shown in Fig. 2. Let the plate radius be R, the lateral velocity of the plate be denoted by $V(r, t)$ and the radial and circumferential rates of curvature be denoted by κ_r and κ_ϕ, respectively. Then

$$V = \frac{\partial W}{\partial t} \tag{2.2}$$

$$\kappa_r = -\frac{\partial^2 V}{\partial r^2}, \tag{2.3}$$

$$\kappa_\phi = -\frac{1}{r}\frac{\partial V}{\partial r}. \tag{2.4}$$

The material of the plate is assumed to be rigid, perfectly plastic, and insensitive to strain rate. The Tresca yield condition of Fig. 3 will be used here. The flow rule states that

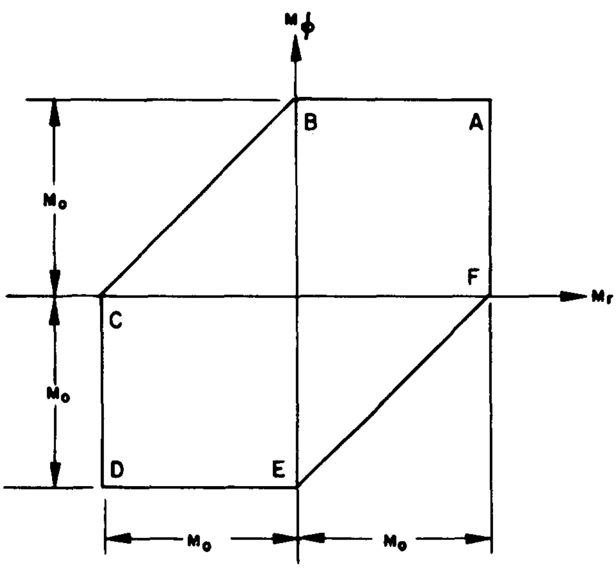

FIG. 3. Tresca yield condition.

the flow vector with components κ_r, κ_ϕ is in the direction of the outward perpendicular to the yield locus at the yield state (M_r, M_ϕ).

The three plastic regimes occurring in the plate under uniform load are point A, segment AB and point B of Fig. 3. From the yield condition and the flow rule, the conditions on the bending moments and rates of curvature for these regimes are:

$$\text{Regime } A: \quad M_r = M_\phi = M_0, \kappa_r \geq 0, \kappa_\phi \geq 0. \tag{2.5}$$

$$\text{Regime } AB: \quad 0 < M_r < M_0, M_\phi = M_0, \kappa_r = 0, \kappa_\phi \geq 0. \tag{2.6}$$

$$\text{Regime } B: \quad M_r = 0, M_\phi = M_0, \kappa_\phi \geq -\kappa_r \geq 0. \tag{2.7}$$

During the plastic deformation of the plate subjected to uniform pressure

$$M_\phi = M_0, \qquad 0 \leq r \leq R. \tag{2.8}$$

The simply supported outer edge of the plate is in regime B; i.e.

$$V = W = M_r = 0 \quad \text{at } r = R. \tag{2.9}$$

For load histories such that no hinge band appears, the center of the plate is in regime A, so that

$$M_r = M_0 \quad \text{at } r = 0, \tag{2.10}$$

while the remainder of the plate is in regime AB, which means, using equations (2.3), (2.4) and (2.6),

$$0 < M_r < M_0, \qquad \frac{\partial^2 V}{\partial r^2} = 0, \qquad \frac{\partial V}{\partial r} \leq 0 \quad \text{for } 0 < r < R. \tag{2.11}$$

If a hinge band of radius $\rho(t)$ grows out from the center of the plate, the entire band is in regime A so that

$$M_r = M_0, \qquad \frac{\partial^2 V}{\partial r^2} \leq 0, \qquad \frac{\partial V}{\partial r} \leq 0 \quad \text{for } 0 \leq r \leq \rho, \tag{2.12}$$

while the remainder of the plate is still in regime AB;

$$0 < M_r < M_0, \qquad \frac{\partial^2 V}{\partial r^2} = 0, \qquad \frac{\partial V}{\partial r} \leq 0 \quad \text{for } \rho < r < R. \tag{2.13}$$

The initial condition of the motion is that the plate is at rest until time t_y when the yield load is first reached. Consequently

$$V(r, t_y) = W(r, t_y) = 0. \tag{2.14}$$

The equation of motion (2.1) must be solved subject to the initial conditions (2.14) and the boundary conditions and restrictions (2.8)–(2.11) if there is no hinge band. If a hinge band appears, equations (2.10) and (2.11) are replaced by equations (2.12) and (2.13).

The restrictions on the continuity of M_r, M_ϕ, W and their derivatives are discussed in detail in [1]. The arguments will not be repeated here; the conclusions pertinent to this problem are: W, V, M_r and $\partial W/\partial r$ are continuous in r and t, but across a moving hinge circle $\rho(t)$ the discontinuity conditions

$$\left\{\frac{\partial V}{\partial r}\right\}+\frac{\mathrm{d}\rho}{\mathrm{d}t}\left\{\frac{\partial^2 W}{\partial r^2}\right\} = 0,$$
$$\left\{\frac{\partial V}{\partial t}\right\}+\frac{\mathrm{d}\rho}{\mathrm{d}t}\left\{\frac{\partial V}{\partial r}\right\} = 0, \tag{2.15}$$
$$\left\{\frac{\partial M_r}{\partial t}\right\}+\frac{\mathrm{d}\rho}{\mathrm{d}t}\left\{\frac{\partial M_r}{\partial r}\right\} = 0,$$

must be satisfied. In equations (A-11), $\{f\}$ denotes the discontinuity in f across ρ.

3. SOLUTION FOR NO HINGE BAND ($P_{max} \leq P_b$)

Guided by the static limit analysis of Hopkins and Prager [19], take the initial velocity distribution as

$$V(r, t) = V_0(t)\left(\frac{R-r}{R}\right), \tag{3.1}$$

where V_0 is the velocity at the plate center. The condition in equations (2.9) that V vanishes at $r = R$ and the conditions on $\partial^2 V/\partial r^2$ and $\partial V/\partial r$ in equations (2.11) are satisfied by equation (3.1). The substitution from equations (2.8), (2.2) and (3.1) into equation (2.1), followed by integration with respect to r and the use of the boundary conditions (2.9) and (2.10) on M_r, results in

$$\frac{\mathrm{d}V_0}{\mathrm{d}t} = \frac{2}{\mu}[P(t)-P_y], \tag{3.2}$$

$$M_r = \frac{(R-r)}{6R}[P(t)r^2+P_y(R^2+Rr-r^2)], \tag{3.3}$$

where the static yield load P_y is

$$P_y = \frac{6M_0}{R^2}. \tag{3.4}$$

The solution of the differential equations (2.2) and (3.2) is, using equation (3.1) and the initial condition (2.14),

$$V_0(t) = \frac{2}{\mu}\int_{t_y}^{t} [P(\tau)-P_y]\,\mathrm{d}\tau, \tag{3.5}$$

$$W_0(t) = \frac{2}{\mu}\int_{t_y}^{t} (t-\tau)[P(\tau)-P_y]\,\mathrm{d}\tau, \tag{3.6}$$

$$W(r, t) = W_0(t)\left(\frac{R-r}{R}\right), \tag{3.7}$$

where $W_0(t)$ is the displacement at the plate center.

Because $M_r = M_0$ and $\partial M_r/\partial r = 0$ at $r = 0$ [see equation (2.1)] the condition that $M_r \leq M_0$ throughout the region $0 < r < R$ will be satisfied if $r = 0$ is a local maximum of M_r; i.e.

$$\frac{\partial^2 M_r}{\partial r^2} < 0 \quad \text{at } r = 0, \tag{3.8}$$

which by equation (3.3) is equivalent to

$$P(t) < 2P_y. \tag{3.9}$$

Define

$$P_b = 2P_y \tag{3.10}$$

as the load at which a hinge band is initiated. The condition that $P(t)$ does not produce a hinge band is then

$$P_{\text{max}} < P_b. \tag{3.11}$$

The plastic deformation ends at time t_f when $V(r, t)$ vanishes. By equations (3.1) and (3.5), t_f is found from the solution of

$$\int_{t_y}^{t_f} P(t)\,\mathrm{d}t = P_y(t_f - t_y). \tag{3.12}$$

Equation (3.12) has the interpretation that the average pressure over the interval of deformation is the yield load.

Define the impulse I per unit area, the mean time t_{mean} of the pulse, and the effective pressure P_e by

$$\begin{aligned} I &= \int_{t_y}^{t_f} P(t)\,\mathrm{d}t, \\ t_{\text{mean}} &= \frac{1}{I}\int_{t_y}^{t_f} (t - t_y)P(t)\,\mathrm{d}t, \\ P_e &= \frac{I}{2t_{\text{mean}}}. \end{aligned} \tag{3.13}$$

The final plastic deformation at $r = 0$ is found from equations (3.6), (3.12) and (3.13) to be

$$W_0(t_f) = \frac{I^2}{\mu P_y}\left(1 - \frac{P_y}{P_e}\right), \tag{3.14}$$

and $W(r, t_f)$ is easily determined from equations (3.7) and (3.14).

4. SOLUTION FOR DEFORMATION WITH HINGE BAND ($P_{\text{max}} > P_b$)

Interval $t_y \leq t \leq t_b$. The solution given by equations (3.3) and (3.5)–(3.7) is applicable up to the time t_b when the pressure first reaches the value P_b and $\partial^2 M_r/\partial r^2 = 0$ at $r = 0$. At t_b a hinge circle $\rho(t)$ separating the region of the plate in regime A from the region in regime AB begins to move out from the origin.

Interval $t_b \le t \le t_{max}$. The substitution from equations (2.8) and (2.12) for M_ϕ and M_r into the partial differential equation (2.1) results in the integral vanishing for arbitrary r in the region $0 \le r \le \rho(t)$. This implies that the integrand must be identically zero, or,

$$\mu \frac{\partial V}{\partial t} = P(t). \tag{4.1}$$

The solution of equation (4.1) is

$$\mu V(r, t) = \int_{t_b}^{t} P(\tau)\,\mathrm{d}\tau + \Omega(r), \qquad 0 \le r \le \rho(t), \tag{4.2}$$

where $\Omega(r)$ is an arbitrary function determined from the continuity of the velocity at the edge of the region. Letting $V_\rho(t)$ be the instantaneous lateral velocity at the hinge circle, i.e.

$$V_\rho(t) = V(\rho(t), t), \tag{4.3}$$

Ω is found from

$$\Omega(\rho) = \mu V_\rho - \int_{t_b}^{t} P(\tau)\,\mathrm{d}\tau, \tag{4.4}$$

where t is viewed as a function of ρ rather than the converse.

Since the integrand in equation (2.1) is identically zero for $0 < r < \rho(t)$, the governing partial differential equation for the region $\rho(t) < r < R$ is, using equations (2.8), (3.4) and (2.2),

$$\frac{\partial}{\partial r}(rM_r) = \frac{1}{6}P_y R^2 + \int_{\rho}^{r}\left[-P(t) + \mu\frac{\partial V}{\partial t}\right] r\,\mathrm{d}r. \tag{4.5}$$

Using the relations (2.13) and (2.9), the expression for $V(r, t)$, analogous to equation (3.1) which applies up to t_b, will be taken as

$$V(r, t) = V_\rho(t)\frac{R-r}{R-\rho(t)}, \qquad \rho \le r \le R, \qquad t_b \le t \le t_c, \tag{4.6}$$

where t_c is the time when the hinge band shrinks to the origin. Integration of equation (4.5) with respect to r and application of the boundary condition on M_r given in equation (2.9) and the continuity of M_r at $r = \rho$ then give

$$\frac{\mathrm{d}}{\mathrm{d}t}\left(\frac{V_\rho}{R-\rho}\right) = \frac{2}{\mu(R-\rho)(R+3\rho)}\left[-\frac{R^3 P_y}{(R-\rho)^2} + (R+2\rho)P\right], \tag{4.7}$$

$$\begin{aligned} M_r = \frac{R-r}{6r(R-\rho)(R+3\rho)}\Bigg[&(R^3 r + R^2 r^2 - Rr^3 - 4R\rho^3 + 3\rho^4)\frac{R^2 P_y}{(R-\rho)^2} \\ &+ (Rr + 2R\rho + 2r\rho + \rho^2)(r-\rho)^2 P\Bigg], \quad \rho \le r \le R, \qquad t_b \le t \le t_c. \end{aligned} \tag{4.8}$$

The condition that M_r should not exceed M_0 in the region $\rho \le r \le R$ implies

$$\frac{\partial^2 M_r}{\partial r^2} \le 0 \quad \text{at } r = \rho^+. \tag{4.9}$$

Using equation (4.8), this is equivalent to

$$(R+\rho)(R-\rho)^2 P \le 2P_y R^3, \qquad t_b \le t \le t_c. \tag{4.10}$$

When the hinge band is initiated, the radius of the hinge circle is zero and the pressure has the value $2P_y$ by equation (3.10). Consequently, the equality in (4.10) holds at $t = t_b$. We will hypothesize that the equality continues to hold in the entire interval $t_b \le t \le t_{\max}$, so that $\rho(t)$ is determined by the solution of the cubic equation

$$[R+\rho(t)][R-\rho(t)]^2 = \frac{2P_y R^3}{P(t)}, \qquad t_b \le t \le t_{\max}. \tag{4.11}$$

The basis of this hypothesis is as follows: the differentiation of equation (4.11) yields

$$\frac{\mathrm{d}\rho}{\mathrm{d}t} = \frac{2P_y R^3}{(R-\rho)(R+3\rho)P^2}\frac{\mathrm{d}P}{\mathrm{d}t}. \tag{4.12}$$

Since $\mathrm{d}\rho/\mathrm{d}t$ and $\mathrm{d}P/\mathrm{d}t$ have the same sign and vanish at the same time, $\rho(t)$ attains its maximum when $P = P_{\max}$. Equations (4.11) and (4.12) imply that the hinge circle is "pushed" out from the origin to its extreme position as the pressure increases from P_b to $P_{\max}$. A value of ρ less than that which satisfies equation (4.11) would cause the inequality (4.10) to be violated. It can be shown that a solution for the plate deformation obtained by using equation (4.11) satisfies the differential equations, boundary conditions and the discontinuity conditions (2.15), and is therefore the correct solution.

Combining equation (4.11) with (4.8) gives

$$\frac{M_r}{M_0} = 1 - \frac{R(r+\rho)(r-\rho)^3}{r(R+\rho)(R-\rho)^3}, \qquad \rho \le r \le R, \qquad t_b \le t \le t_{\max}, \tag{4.13}$$

while equation (4.7) reduces to

$$\frac{\mathrm{d}}{\mathrm{d}t}\left(\frac{V_\rho}{R-\rho}\right) = \frac{P}{\mu(R-\rho)}. \tag{4.14}$$

We integrate equation (4.14) to obtain

$$V_\rho(t) = [R-\rho(t)]\left[\frac{1}{\mu}\int_{t_b}^{t}\frac{P(\tau)}{R-\rho(\tau)}\,\mathrm{d}\tau + \frac{V_\rho(t_b)}{R-\rho(t_b)}\right]. \tag{4.15}$$

Since $V_\rho(t_b) = V_0(t_b)$ and $\rho(t_b) = 0$, we have from equation (3.5) that

$$V_\rho(t_b) = \frac{2}{\mu}\int_{t_y}^{t_b}[P(\tau)-P_y]\,\mathrm{d}\tau. \tag{4.16}$$

Substituting from equations (4.15) and (4.16) into equation (4.6) gives

$$V(r,t) = \frac{R-r}{\mu R}\left[R\int_{t_b}^{t}\frac{P(\tau)}{R-\rho(\tau)}\,\mathrm{d}\tau + 2\int_{t_y}^{t_b}[P(\tau)-P_y]\,\mathrm{d}\tau\right], \qquad \rho \le r \le R, \qquad t_b \le t \le t_{\max}. \tag{4.17}$$

The plate displacement is then found by integrating the velocity and applying the continuity conditions at t_b, using equations (3.6) and (3.7). The result is

$$W(r,t) = \frac{R-r}{\mu R}\left\{R\int_{t_b}^{t}\frac{(t-\tau)P(\tau)}{R-\rho(\tau)}\,\mathrm{d}\tau + 2\int_{t_y}^{t_b}(t-\tau)[P(\tau)-P_y]\,\mathrm{d}\tau\right\},$$
$$\rho \le r \le R, \qquad t_b \le t \le t_{max}. \tag{4.18}$$

We return now to the region $0 \le r \le \rho$ in order to determine $\Omega(r)$ from the continuity of the velocity at the hinge circle. The solution $\rho(t)$ to equation (4.11) can be inverted to give

$$t = \beta(\rho), \qquad 0 \le \rho \le \rho_{max}, \qquad t_b \le t \le t_{max} \tag{4.19}$$

with

$$\beta(\rho) = P^{-1}\left[\frac{2P_yR^3}{(R+\rho)(R-\rho)^2}\right], \qquad P_b \le P(t) \le P_{max}. \tag{4.20}$$

By equations (4.4), (4.15), (4.16) and (4.19), we have

$$\Omega(\rho) = (R-\rho)\left[\int_{t_b}^{\beta(\rho)}\frac{P(\tau)}{R-\rho(\tau)}\,\mathrm{d}\tau + 2\int_{t_y}^{t_b}[P(\tau)-P_y]\,\mathrm{d}\tau\right]$$
$$-\int_{t_b}^{\beta(\rho)}P(\tau)\,\mathrm{d}\tau, \qquad 0 \le \rho \le \rho_{max}. \tag{4.21}$$

Substituting this result into equation (4.2) then gives

$$\mu V(r,t) = \int_{\beta(r)}^{t}P(\tau)\,\mathrm{d}\tau + (R-r)\int_{t_b}^{\beta(r)}\frac{P(\tau)}{R-\rho(\tau)}\,\mathrm{d}\tau$$
$$+\frac{2(R-r)}{R}\int_{t_y}^{t_b}[P(\tau)-P_y]\,\mathrm{d}\tau, \qquad 0 \le r \le \rho, \qquad t_b \le t \le t_c. \tag{4.22}$$

The displacement is found by integrating $V(r,t)$ with respect to time and applying continuity conditions at $t = t_b$; the result is

$$\mu W(r,t) = \int_{\beta(r)}^{t}(t-\tau)P(\tau)\,\mathrm{d}\tau + (R-r)\int_{t_b}^{\beta(r)}\frac{(t-\tau)P(\tau)}{R-\rho(\tau)}\,\mathrm{d}\tau$$
$$+\frac{2(R-r)}{R}\int_{t_y}^{t_b}(t-\tau)[P(\tau)-P_y]\,\mathrm{d}\tau, \tag{4.23}$$
$$0 \le r \le \rho, \qquad t_b \le t \le t_c.$$

The upper limit of the interval of applicability of these last two equations is t_c rather than t_{max} as will be explained in the next section.

In summary for the interval $t_b \le t \le t_{max}$, the hinge circle radius is found from equation (4.11), and the plate velocity and displacement are given by equations (4.22) and (4.23), respectively, in the interior of the hinge band and by equations (4.17) and (4.18) in the exterior region. Performing the required differentiation on either side of the hinge circle, it can be shown that the discontinuity conditions (2.15) are satisfied; in fact, all the derivatives appearing in equations (2.15) are continuous at the hinge circle. Properly speaking, $\rho(t)$ should be referred to as a plastic regime boundary in the interval $t_b \le t \le t_{max}$ since the term "hinge circle" implies a discontinuity in $\partial V/\partial r$ at ρ. However, such a discontinuity occurs for $t_{max} \leq t \leq t_c$ so that ρ is both a hinge circle and a regime boundary in the latter interval. Consequently, there seems little point in making the distinction in terminology.

Since $\beta(0) = t_b$, we have from equations (4.22) and (4.23) that the velocity and displacement at the center of the plate are given by

$$\mu V_0(t) = \int_{t_b}^{t} P(\tau)\,\mathrm{d}\tau + 2\int_{t_y}^{t_b} [P(\tau) - P_y]\,\mathrm{d}\tau,$$

$$\mu W_0(t) = \int_{t_b}^{t} (t-\tau)P(\tau)\,\mathrm{d}\tau + 2\int_{t_y}^{t_b} (t-\tau)[P(\tau) - P_y]\,\mathrm{d}\tau, \tag{4.24}$$

$$t_b \leq t \leq t_c.$$

Interval $t_{max} \leq t \leq t_c$. Equations (4.1)–(4.10) remain applicable for this time interval. However, making the assumption that $\rho(t)$ is still given by equation (4.11) would produce results which would violate the discontinuity conditions (2.15). Since $\rho(t)$ now starts to move back toward the origin, the function $\Omega(r)$ is known for every position $r \leq \rho$ which occurs during this time interval. Consequently equations (4.22) and (4.23) are still valid for the velocity and displacement inside the hinge band, as are equations (4.24) for the central velocity and displacement. We must still determine $\rho(t)$ and the velocity and displacement outside the hinge band.

Letting $r = \rho$ in equation (4.22), we can write

$$\frac{\mu V_\rho(t)}{R-\rho} = \frac{1}{R-\rho}\int_{\beta(\rho)}^{t} P(\tau)\,\mathrm{d}\tau + \int_{t_b}^{\beta(\rho)} \frac{P(\tau)}{R-\rho(\tau)}\,\mathrm{d}\tau$$
$$+\frac{2}{R}\int_{t_y}^{t_b} [P(\tau) - P_y]\,\mathrm{d}\tau, \tag{4.25}$$

$$t_{max} \leq t \leq t_c.$$

Differentiating equation (4.25) with respect to time gives

$$\mu\frac{\mathrm{d}}{\mathrm{d}t}\left(\frac{V_\rho}{R-\rho}\right) = \frac{\mathrm{d}\rho}{\mathrm{d}t}\frac{1}{(R-\rho)^2}\int_{\beta(\rho)}^{t} P(\tau)\,\mathrm{d}\tau + \frac{P(t)}{R-\rho}. \tag{4.26}$$

Eliminating $\mathrm{d}/\mathrm{d}t(V_\rho/R-\rho)$ between equations (4.7) and (4.26) then gives a differential equation for ρ; this equation is, after some algebraic manipulation,

$$\frac{\mathrm{d}\rho}{\mathrm{d}t}(R-\rho)(R+3\rho)\int_{\beta(\rho)}^{t} P(\tau)\,\mathrm{d}\tau - P(t)(R+\rho)(R-\rho)^2 + 2P_yR^3 = 0. \tag{4.27}$$

Observing that

$$\frac{\mathrm{d}}{\mathrm{d}\rho}[(R+\rho)(R-\rho)^2] = -(R-\rho)(R+3\rho), \tag{4.28}$$

we can integrate equation (4.27). Using the continuity conditions at t_{max}, we find that the equation which determines $\rho(t)$ is therefore

$$\int_{\beta(\rho)}^{t} P(\tau)\,\mathrm{d}\tau = \frac{2P_yR^3[t-\beta(\rho)]}{(R+\rho)(R-\rho)^2}, \qquad t_{max} \leq t \leq t_c. \tag{4.29}$$

The hinge circle motion ceases at t_c when $\rho = 0$. Since, by equation (4.19), $\beta(0) = t_b$, the time t_c is found from equation (4.29) to be determined by solving

$$\int_{t_b}^{t_c} P(t)\,\mathrm{d}t = P_b(t_c - t_b). \tag{4.30}$$

The last equation has the interpretation that the average pressure over the interval when the hinge band exists is the pressure at which the band is initiated.

The velocity distribution outside the hinge band region is found from equations (4.6) and (4.25) to be

$$\mu V(r,t) = \frac{R-r}{R-\rho}\int_{\beta(\rho)}^{t} P(\tau)\,\mathrm{d}\tau + (R-r)\int_{t_b}^{\beta(\rho)} \frac{P(\tau)}{R-\rho(\tau)}\,\mathrm{d}\tau + \frac{2(R-r)}{R}\int_{t_y}^{t_b}[P(\tau)-P_y]\,\mathrm{d}\tau, \qquad \rho(t) \le r \le R, \qquad t_{\max} \le t \le t_c. \tag{4.31}$$

A derivation of the deformation profile in the region $\rho \le r \le R$ is given in Ref. [5] and will not be repeated here.

The discontinuity conditions (2.15) are satisfied in the interval $t_{\max} \le t \le t_c$. Unlike the previous interval, a discontinuity in $\partial V/\partial r$ occurs at ρ, so ρ is properly called a hinge circle. From equations (4.8) and (4.27), we have that

$$\left.\frac{\partial^2 M_r}{\partial r^2}\right|_{r=\rho^+} = \frac{1}{R-\rho}\frac{\mathrm{d}\rho}{\mathrm{d}t}\int_{\beta(\rho)}^{t} P\,\mathrm{d}\tau. \tag{4.32}$$

Since ρ decreases in this time interval and the integral is non-negative, the inequality (4.9) holds and the yield condition is not violated in the region $\rho \le r \le R$.

Interval $t_c \le t \le t_f$. Since the hinge band has disappeared, equations (3.1)–(3.3) apply in this interval as they did in the initial interval $t_y \le t \le t_b$. After performing straightforward integrations with respect to time we have

$$\begin{aligned}
\mu V(r,t) &= \frac{2(R-r)}{R}\int_{t_y}^{t}[P(\tau)-P_y]\,\mathrm{d}\tau,\\
\mu W(r,t) &= \frac{2(R-r)}{R}\left\{\int_{t_y}^{t}(t-\tau)[P(\tau)-P_y]\,\mathrm{d}\tau - \int_{t_y}^{t_c}(t_c-\tau)[P(\tau)-P_y]\,\mathrm{d}\tau\right\} + \mu W(r,t_c),\\
&\qquad 0 \le r \le R, \qquad t_c \le t \le t_f.
\end{aligned} \tag{4.33}$$

In particular, using the second of equations (4.24), we have

$$\begin{aligned}
\mu V_0(t) &= 2\int_{t_y}^{t}[P(\tau)-P_y]\,\mathrm{d}\tau,\\
\mu W_0(t) &= 2\int_{t_y}^{t}(t-\tau)[P(\tau)-P_y]\,\mathrm{d}\tau - 2\int_{t_b}^{t_c}(t_c-\tau)[P(\tau)-P_y]\,\mathrm{d}\tau\\
&\quad + \int_{t_b}^{t_c}(t_c-\tau)P(\tau)\,\mathrm{d}\tau, \qquad t_c \le t \le t_f.
\end{aligned} \tag{4.34}$$

The time t_f is when the plate deformation ceases; therefore by the first of equations (4.33), t_f is determined from equation (3.12) again.

Evaluating $W_0(t_f)$ from equation (4.34), using equations (4.30) and (3.12), we have, after some algebraic rearrangement,

$$\begin{aligned}\mu W_0(t_f) = {} & \frac{1}{P_y}\left[\int_{t_y}^{t_f} P(t)\,\mathrm{d}t\right]^2 - \frac{1}{4P_y}\left[\int_{t_b}^{t_c} P(t)\,\mathrm{d}t\right]^2 \\ & -2\int_{t_y}^{t_f}(t-t_y)P(t)\,\mathrm{d}t + \int_{t_b}^{t_c}(t-t_b)P(t)\,\mathrm{d}t.\end{aligned} \tag{4.35}$$

Define I^*, t^*_{mean} and P^*_e by

$$\begin{aligned} I^* &= \int_{t_b}^{t_c} P(t)\,\mathrm{d}t, \\ t^*_{\text{mean}} &= \frac{1}{I^*}\int_{t_b}^{t_c}(t-t_b)P(t)\,\mathrm{d}t, \\ P^*_e &= \frac{I^*}{2t^*_{\text{mean}}}. \end{aligned} \tag{4.36}$$

Then from equations (4.35), (4.36) and (3.13) we have

$$W_0(t_f) = \frac{I^2}{\mu P_y}\left[1-\frac{P_y}{P_e}-\frac{1}{2}\left(\frac{I^*}{I}\right)^2\left(\frac{1}{2}-\frac{P_y}{P^*_e}\right)\right]. \tag{4.37}$$

5. RESULTS

In the load range $P_y \le P_{\max} \le 2P_y$, equation (3.14) shows that† $W_0(t_f)/I^2$ is just a function of the effective pressure P_e. For very large peak values of the pressure, $I^* \to I$ and $P^*_e \to P_e$. Consequently, from equation (4.37)

$$W_0(t_f) \to \frac{I^2}{\mu P_y}\left(\frac{3}{4}-\frac{P_y}{2P_e}\right) \quad \text{as } P_{\max} \to \infty. \tag{5.1}$$

The final plastic deformation was calculated from equations (3.14) and (4.37) for various families of pulse shapes defined by:

Rectangular

$$P = P_{\max}, \qquad 0 \le t \le t_1, \qquad P = 0, \qquad t > t_1. \tag{5.2}$$

Linear decay

$$P = \left(1-\frac{t}{t_2}\right)P_{\max}, \qquad 0 \le t \le t_2, \qquad P = 0, \qquad t > t_2. \tag{5.3}$$

Exponential decay

$$P = P_{\max}\,\mathrm{e}^{-t/t_3}, \qquad t \ge 0. \tag{5.4}$$

† Dividing $W_0(t_f)$ by I^2 eliminates the effect of the arbitrary time scale factor inherent in plasticity problems.

Triangular

$$P = \frac{2t}{t_4} P_{\max}, \qquad 0 \le t \le \tfrac{1}{2}t_4,$$

$$P = 2\left(1 - \frac{t}{t_4}\right) P_{\max}, \qquad \tfrac{1}{2}t_4 < t \le t_4, \tag{5.5}$$

$$P = 0, \qquad t > t_4.$$

Half-sine

$$P = P_{\max} \sin\left(\frac{\pi t}{t_5}\right), \qquad 0 \le t \le t_5, \tag{5.6}$$

$$P = 0, \qquad t > t_5.$$

The effective pressures for each of these pulse shape families are computed from equations (3.13), using equation (3.12) to find t_f; the results are shown in Fig. 4 as a function of peak pressure. For pulses which produce hinge bands ($P_{\max} > P_b$), I^* and P_e^* are computed from equations (4.36), using equation (4.30) to evaluate t_c.

The effect of pulse shape on the final plastic deformation of the plate is illustrated in Figs. 5 and 6. The results are shown in Fig. 5 as a function of $P_{\max}$ and in Fig. 6 as a function of P_e. We see that there is a strong dependence on the pulse shape if $P_{\max}$ is used to characterize the pulse, especially for peak loads in the vicinity of P_y. However, the pulse shape effect is essentially eliminated if the effective pressure P_e is used to characterize the pulse shape.

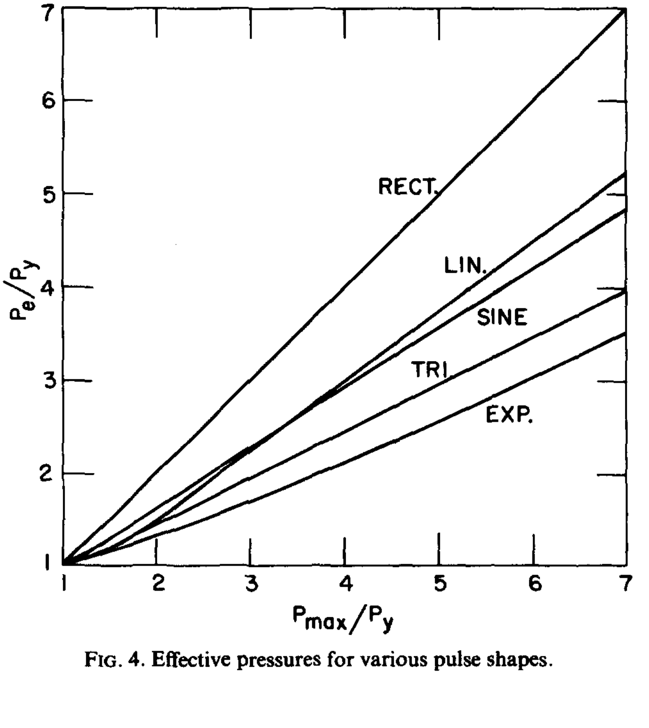

FIG. 4. Effective pressures for various pulse shapes.

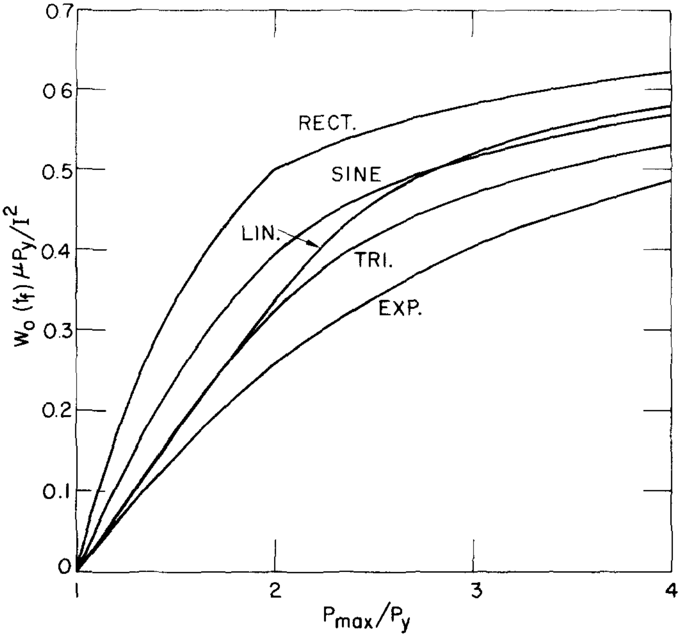

FIG. 5. Maximum deformation as a function of the maximum pressure for various pulse shapes.

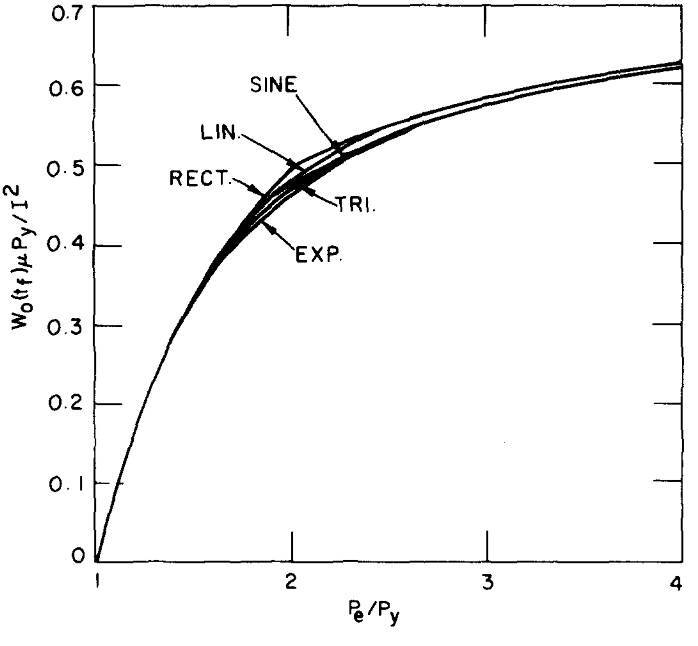

FIG. 6. Maximum deformation as a function of the effective pressure for various pulse shapes.

6. CONCLUSIONS

A closed-form solution has been obtained for the dynamic plastic deformation of a simply-supported circular plate made of a rigid, perfectly plastic material and loaded by the general pulse of Fig. 2. It is shown that the final plastic deformation, which is a functional of the pulse shape, cannot be viewed as a function of the peak pressure and impulse. However, the final plastic deformation can be considered to be a function of the impulse and an *effective* pressure defined in equations (3.13). This is particularly encouraging for experimental applications since the effective pressure depends only on simple integrals of the pulse and is consequently insensitive to inaccuracies in pressure–time measurements.

Another interesting result of the analysis is provided by equations (3.12) and (4.30). From these equations it can be concluded that the average pressure over the interval of plastic deformation is the yield pressure and the average pressure over the interval of hinge band existence is the pressure which produces the band. These time intervals thus may be predicted *a priori* from the pulse shape without determining the deformation history. Experimental verification of these relations again would appear to be relatively straightforward.

REFERENCES

[1] H. G. Hopkins and W. Prager, On the dynamics of plastic circular plates. *Z. angew. Math. Phys.* **5**, 317–330 (1954).
[2] P. P. Perzyna, Dynamic load carrying capacity of a circular plate. *Arch. Mech. stosow.* **10**, 635–647 (1958).
[3] P. G. Hodge, Jr., The influence of blast characteristics on the final deformation of circular cylindrical shells. *J. appl. Mech.* **23**, 617–624 (1956).
[4] P. S. Symonds, Dynamic load characteristics in plastic bending of beams. *J. appl. Mech.* **20**, 475–481 (1953).
[5] C. K. Youngdahl, Load Equivalence Parameters for Dynamic Loading of Structures in the Plastic Range, Argonne National Laboratory Report ANL-7677 (1970).
[6] A. J. Wang, The permanent deflection of a plastic plate under blast loading. *J. appl. Mech.* **22**, 375–376 (1955).
[7] N. Perrone, Impulsively loaded strain-rate-sensitive plates. *J. appl. Mech.* **34**, 380–384 (1967).
[8] T. Wierzbicki, Impulsive loading of rigid viscoplastic plates. *Int. J. Solids Struct.* **3**, 635–647 (1967).
[9] N. Jones, Impulsive loading of a simply supported circular rigid plastic plate. *J. appl. Mech.* **35**, 59–65 (1968).
[10] M. F. Conroy, Rigid-plastic analysis of a simply-supported circular plate due to dynamic circular loading. *J. Franklin Inst.* **288**, 121–135 (1969).
[11] A. L. Florence, Clamped circular rigid-plastic plates under central blast loading. *Int. J. Solids Struct.* **2**, 319–335 (1966).
[12] A. J. Wang and H. G. Hopkins, On the plastic deformation of built-in circular plates under impulsive load. *J. Mech. Phys. Solids* **3**, 22–37 (1954).
[13] G. S. Shapiro, On a rigid-plastic annular plate under impulsive load. *Prikl. Mat. Mek.* **23**, 234–241 (1959).
[14] N. Jones, Finite deflections of a simply supported rigid-plastic annular plate loaded dynamically. *Int. J. Solids Struct.* **4**, 593–603 (1968).
[15] N. Jones, Finite deflections of a rigid-viscoplastic strain-hardening annular plate loaded impulsively. *J. appl. Mech.* **35**, 349–356 (1968).
[16] A. L. Florence, Circular plates under a uniformly distributed impulse. *Int. J. Solids Struct.* **2**, 37–47 (1966).
[17] T. A. Duffey and S. W. Key, Experimental–theoretical correlations of impulsively loaded clamped circular plates. *Exp. Mech.* **9**, 241–249 (1969).
[18] T. Wierzbicki and A. L. Florence, A theoretical and experimental investigation of impulsively loaded clamped circular viscoplastic plates. *Int. J. Solids Struct.* **6**, 553–568 (1970).
[19] H. G. Hopkins and W. Prager, The load carrying capacity of circular plates. *J. Mech. Phys. Solids* **2**, 1–13 (1953).

(*Received* 14 *August* 1970; *revised* 4 *January* 1971)

Абстракт—Получается решение в замкнутом виде для динамической пластической деформации, свободно опертой круглой пластинки, подверженной действию импульса давлени общей формы. Указано, что остаточная пластическая деформация очень зависит от формы импульса. Но даже, эффект формы импульса можно характеризовать эффективным давдением, описанным в виде иросмых цнмеираиов фчнкцм чаьиемия ц ьреиеим.